Supplementary Information: Application of a regularized Coulomb sliding law to Jakobshavn Isbræ, West Greenland

Matt Trevers[1], Anthony Payne[1], and Stephen Cornford[1]

[1]University of Bristol

Correspondence: Matt Trevers (matt.trevers@bristol.ac.uk)
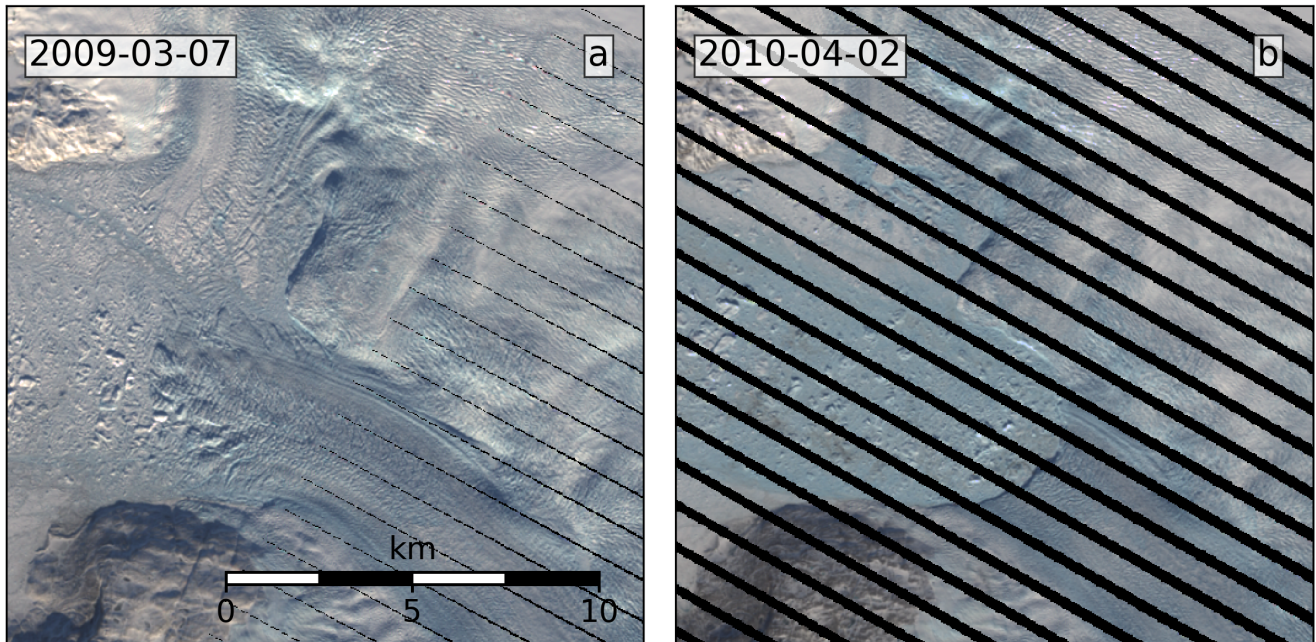
Figure S1. Landsat 7 true-colour images of the glacier terminus from March 7th 2009 (a) and April 2nd 2010 (b). The 2009 image shows the loosely bonded floating sikussak protruding into the fjord. This feature is missing from the 2010 image. Black stripes are artifacts from the Landsat image.
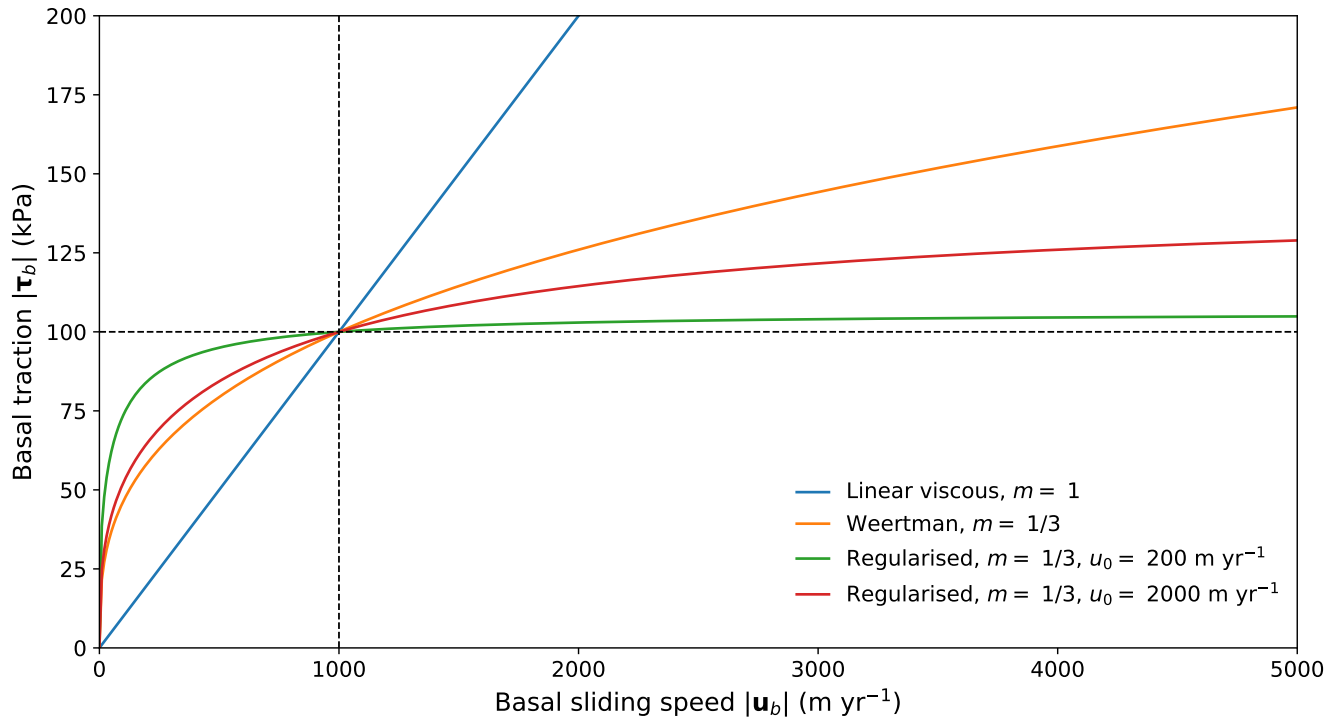
Figure S2. Basal traction plotted as a function of the sliding speed for different sliding laws. Values of the basal friction coefficient C were chosen such that the traction has a value of 100 kPa for a sliding speed of 1000 m yr^{-1}. Figure adapted from Joughin et al. (2019, Fig. 1) but using different parameter values.
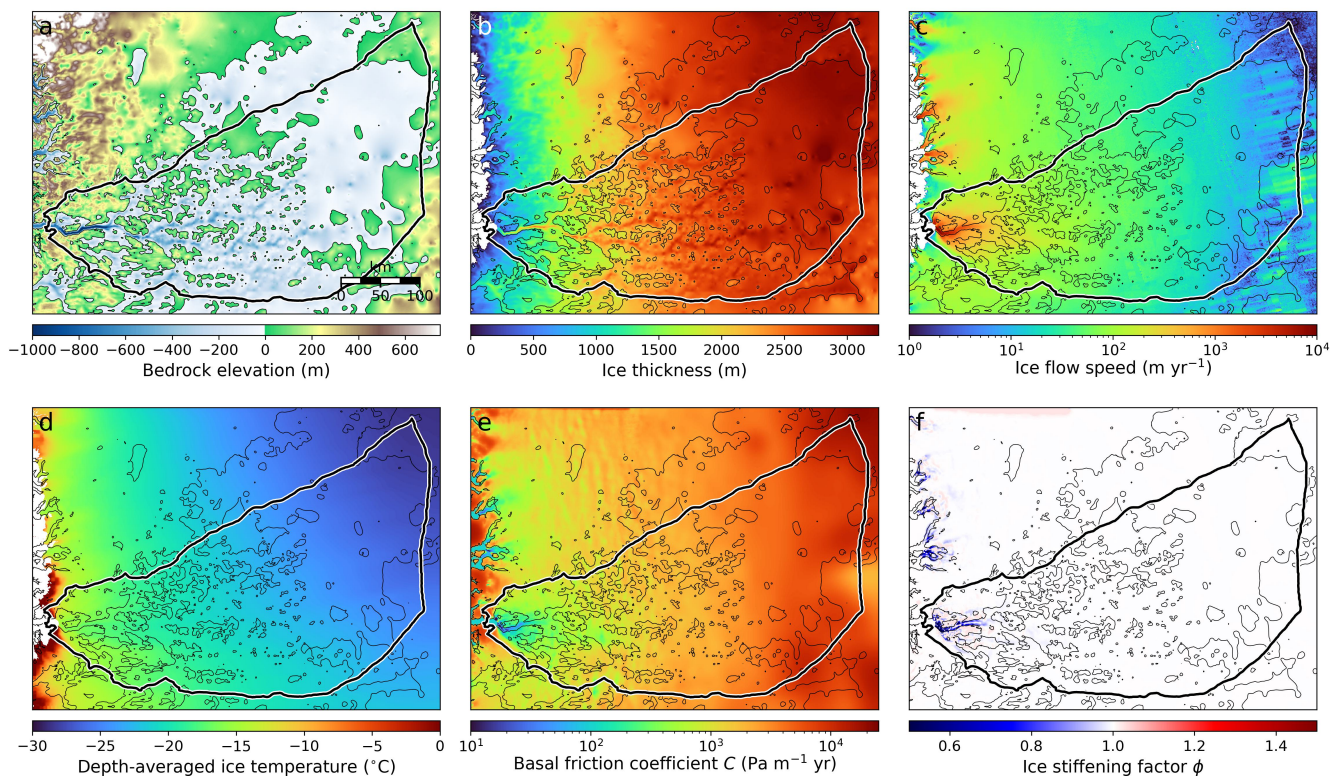
Figure S3. Inverse model inputs for the initial reference timeslice for the full model domain. (a) Bedrock topography (BedMachine v3,) (b) ice thickness (BedMachine v3,) (c) 2008 and 2009 mean ice flow speed (Rignot and Mouginot, 2012, v4), (d) ice temperature, (e) basal friction coefficient and (f) ice stiffening factor. Thin contours delineate the sea level bedrock elevation contour while the thick black line marks the drainage basin boundary.

Dataset	Source	Time range	Resolution	α_u^2
International Polar Year GrIS Velocity (Rignot and Mouginot, 2012, v4)	Envisat RADARSAT-1	2008 to 2009 Initial reference timeslice	150 m	1
MEaSUREs Greenland Ice Velocity: Selected Glacier Site Velocity Maps from InSAR (Joughin et al., 2020, NSIDC-0481, v2)	TerraSAR-X	2008 to present 11 day repeat period	100 m	2
MEaSUREs GrIS Velocity Map from InSAR (Joughin et al., 2018, NSIDC-0478, v2)	RADARSAT-1 Sentinel-1 TerraSAR-X	Annual: 2009, 2010, 2012 - 2017 Quarterly: 2009, 2010, 2012, 2013	500 m	1
MEaSUREs GrIS Monthly Velocity Mosaics from SAR and Landsat (Joughin, 2019, NSIDC-0731, v1)	Landsat-8 Sentinel-1 TerraSAR-X	Dec 2014 to present	200 m	1

Table S1. Details of velocity datasets assimilated in the time-dependent inverse model on a quarterly or annual basis.
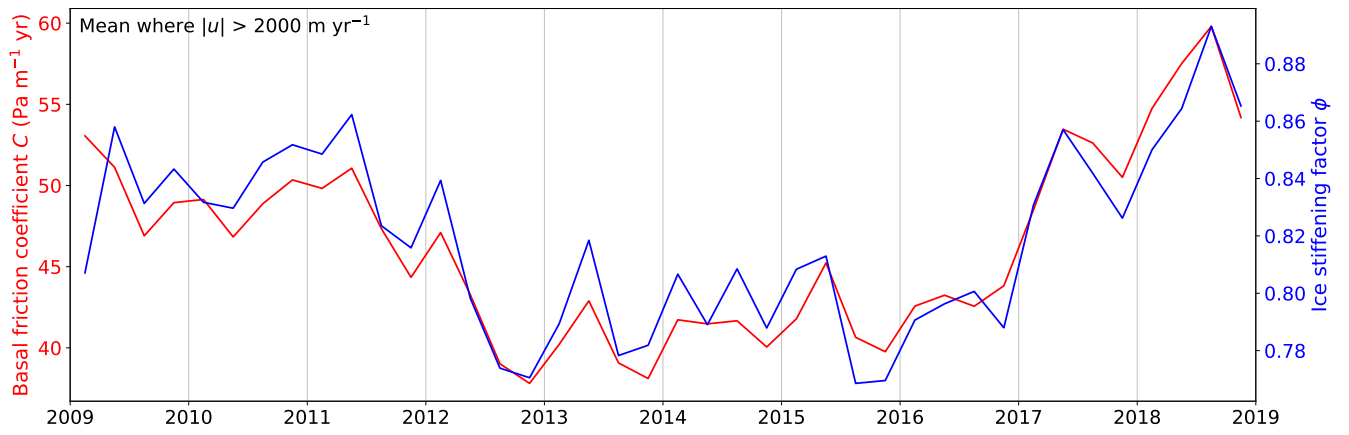
Figure S4. time-series of quarterly C and ϕ, averaged across the region where the flow speed was always in excess of 2000 m yr^{-1}.
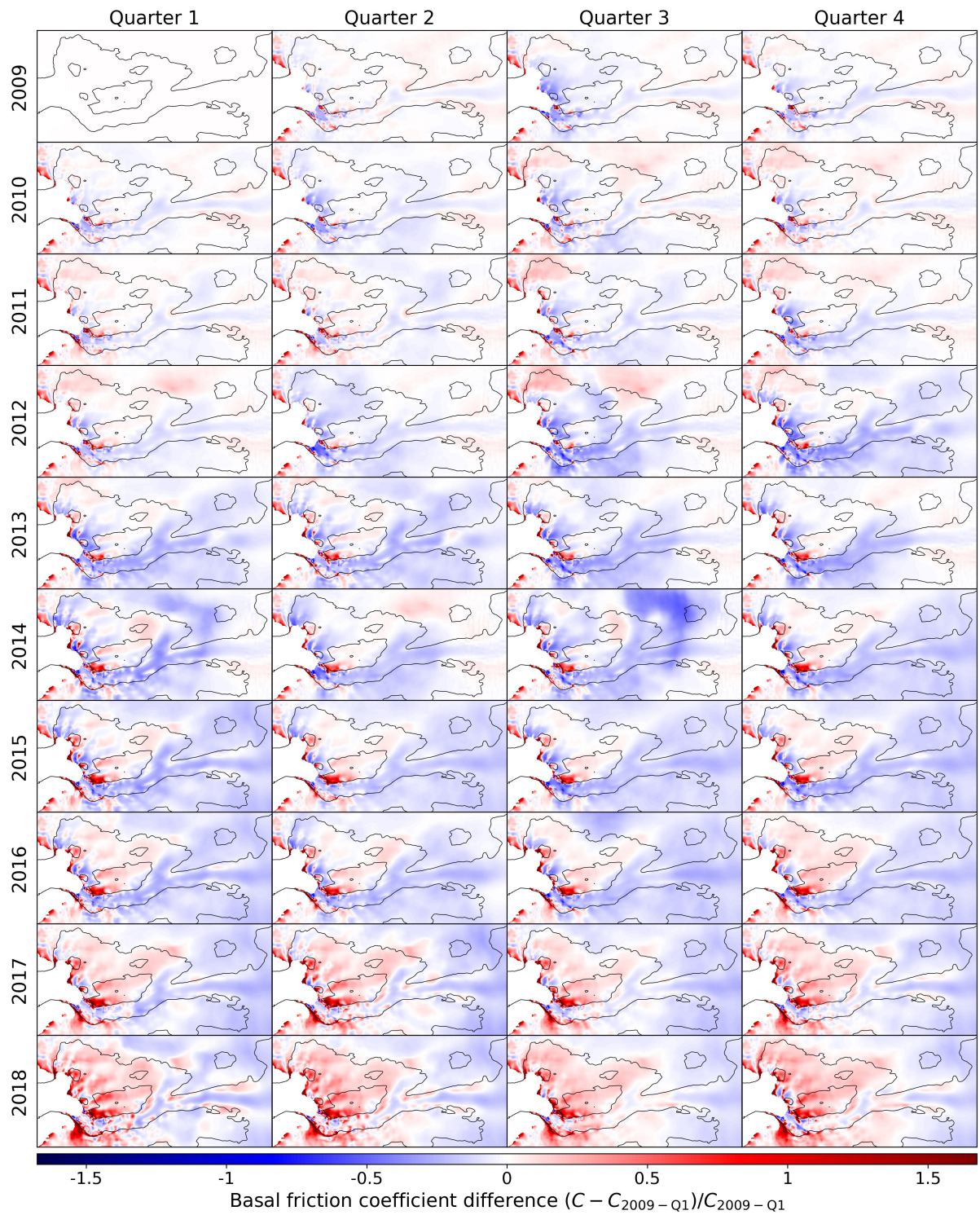
Figure S5. Relative difference in the basal friction coefficient C for each quarterly timeslice compared with the 2009-Q1 timeslice for the ice stream region of the domain.
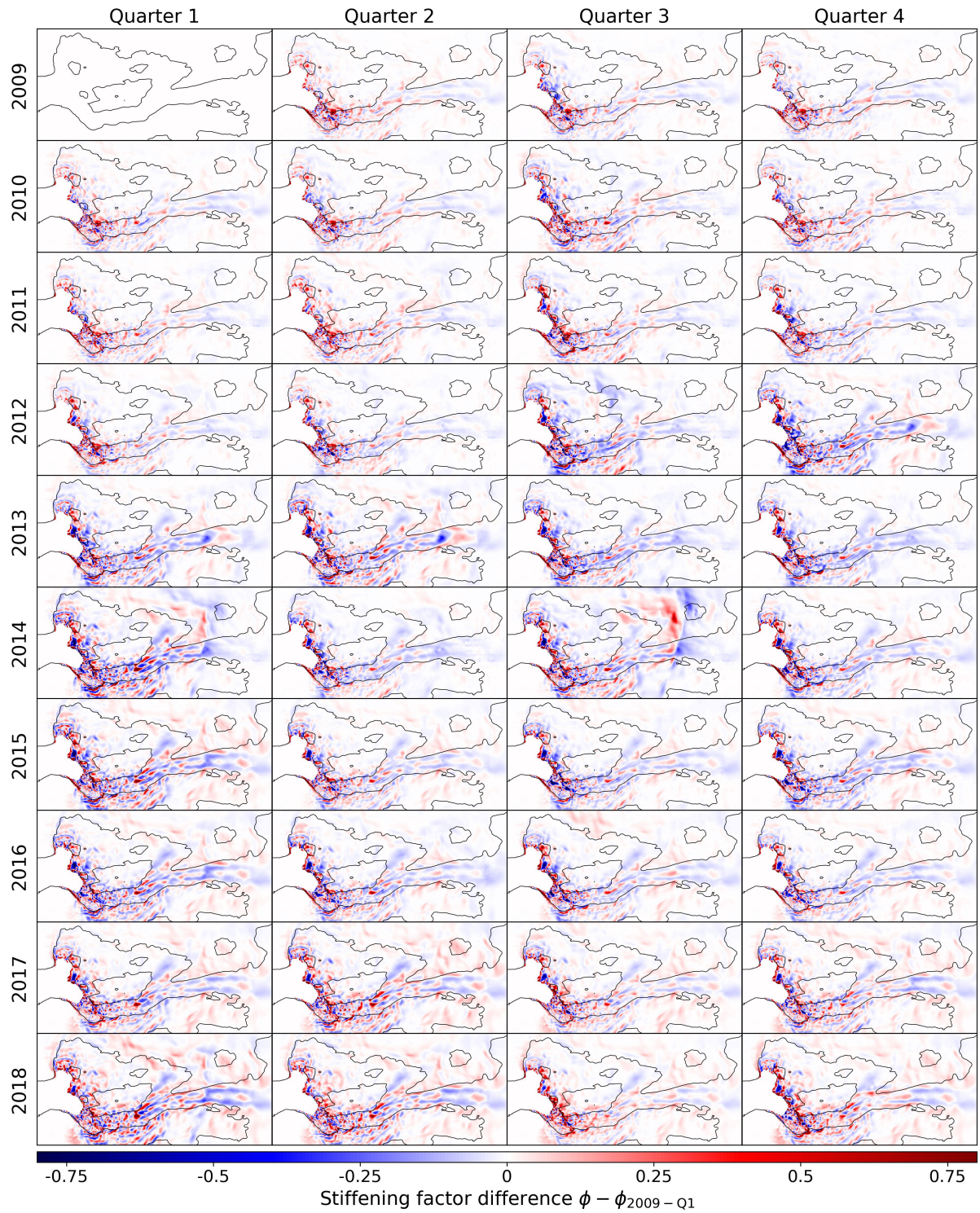
Figure S6. Difference of the stiffening factor ϕ for each quarterly timeslice compared with the 2009-Q1 timeslice for the ice stream region of the domain.
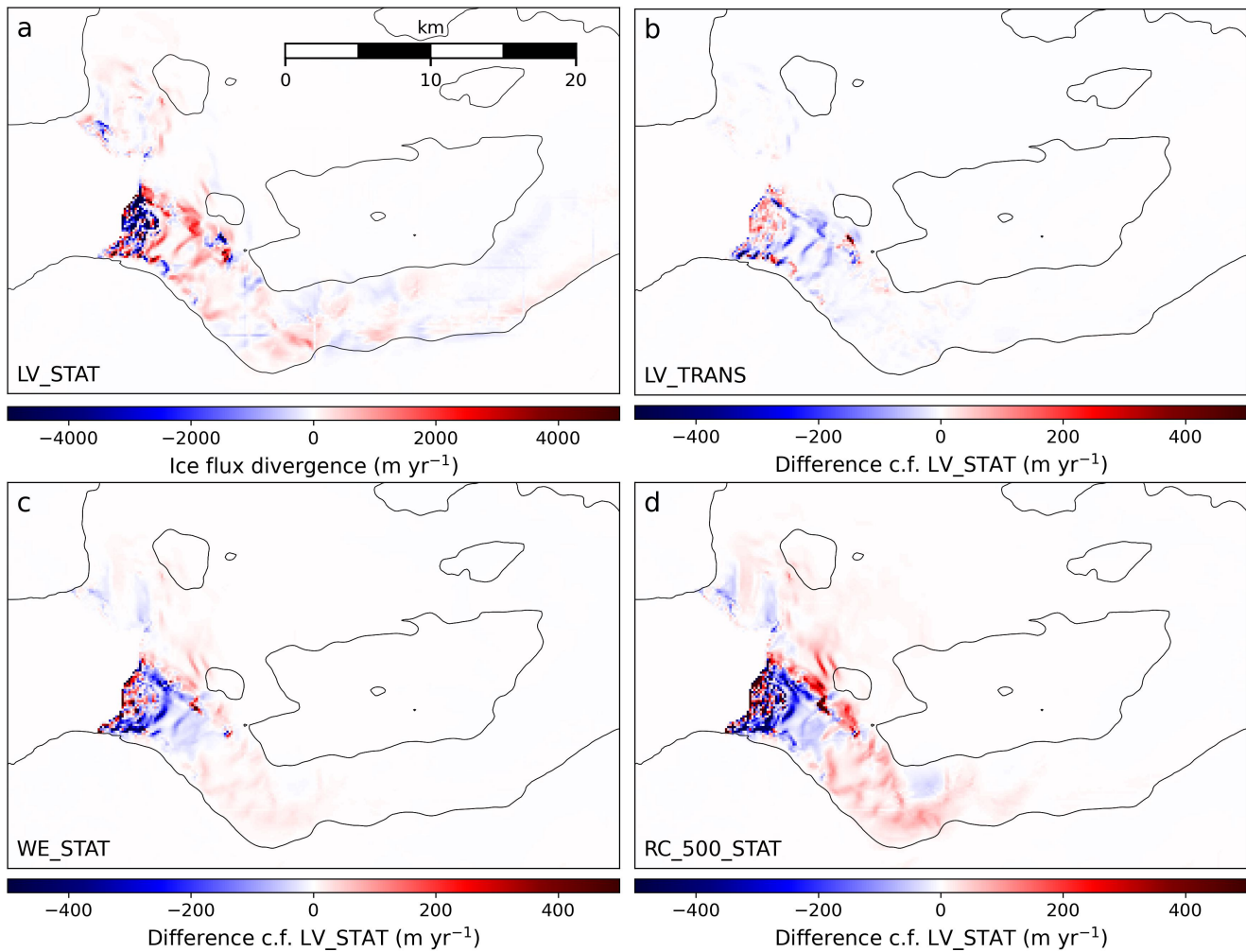
Figure S7. Ice flux divergence $\nabla\left(uh\right)$ at the start of hindcast model simulations. (a) Ice flux divergence for the LV_STAT experiment. (b) to (d) Difference in ice flux divergence relative to LV_STAT for the LV_TRANS, WE_STAT and RC_500_STAT experiments respectively.
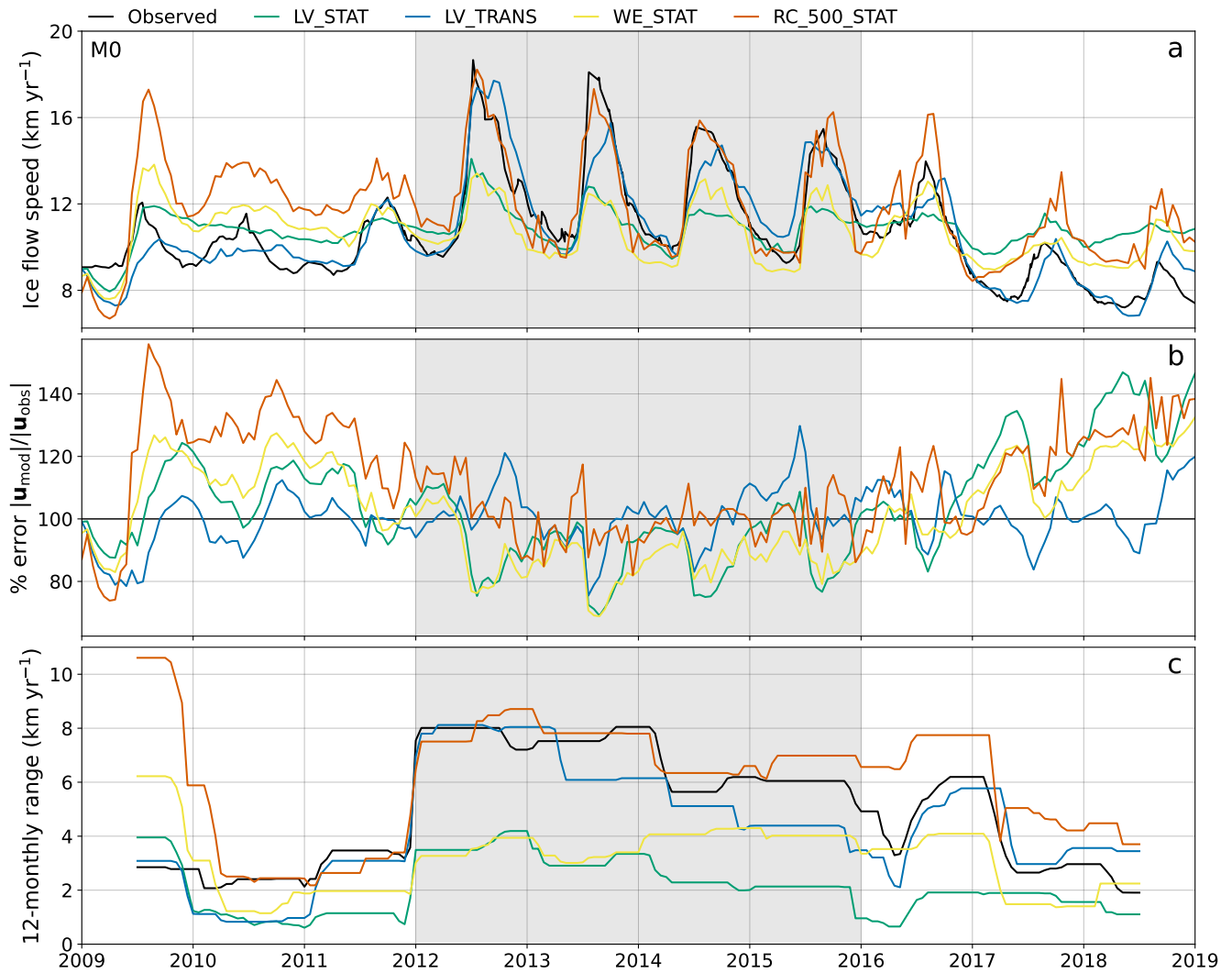
Figure S8. Modelled flow speeds in the hindcast simulations measured at site M0. (a) Observed (black line) and modelled (coloured lines) ice flow speeds. (b) Percentage error in modelled flow speeds. (c) Rolling 12-monthly velocity range. The 12-monthly range is calculated as the difference between maximum and minimum flow speeds within 6 months either side of the measurement. Panel (a) is identical to Figure 4 in the main text.
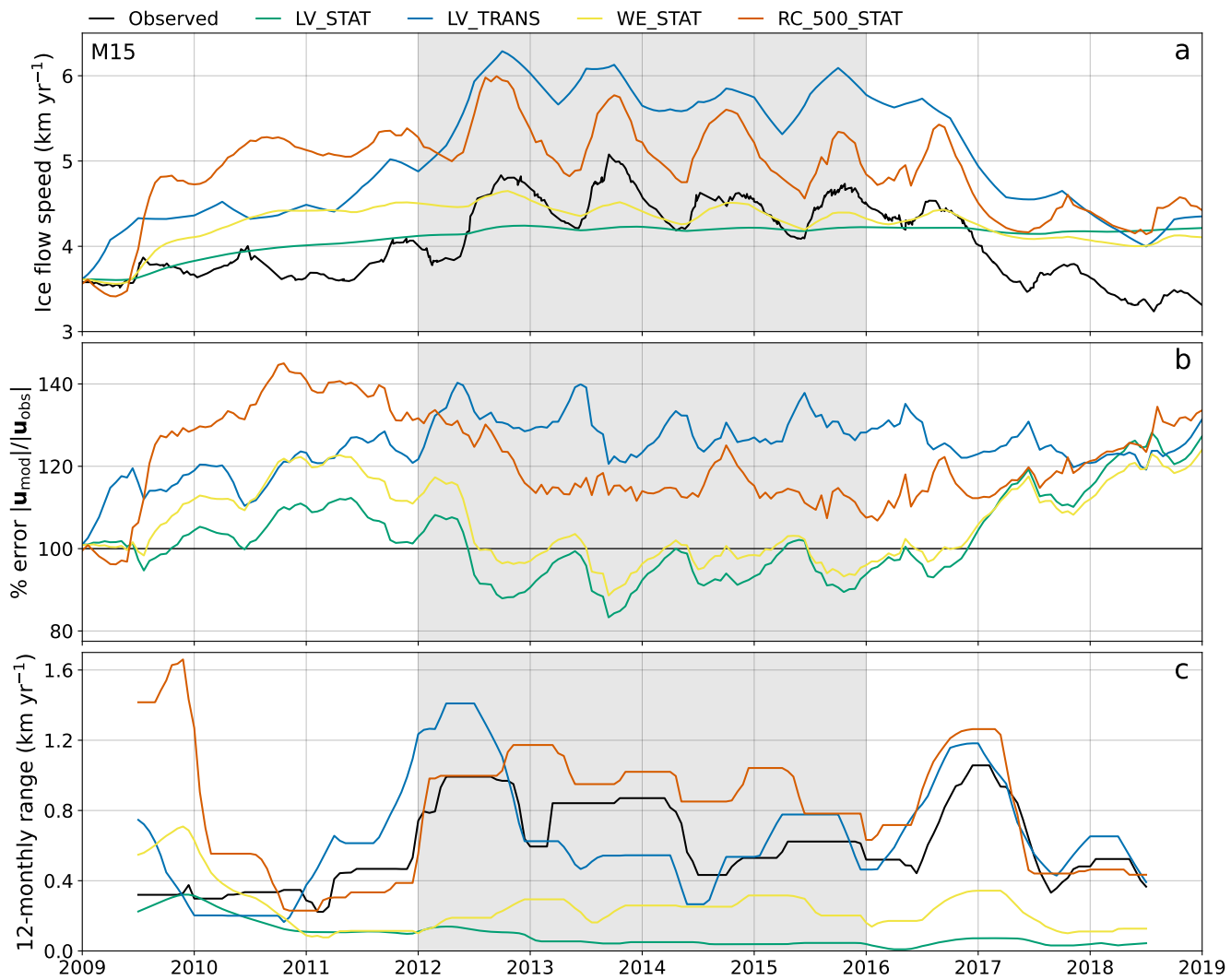
Figure S9. Modelled flow speeds in the hindcast simulations measured at site M15. (a) to (c) as in Figure S8.
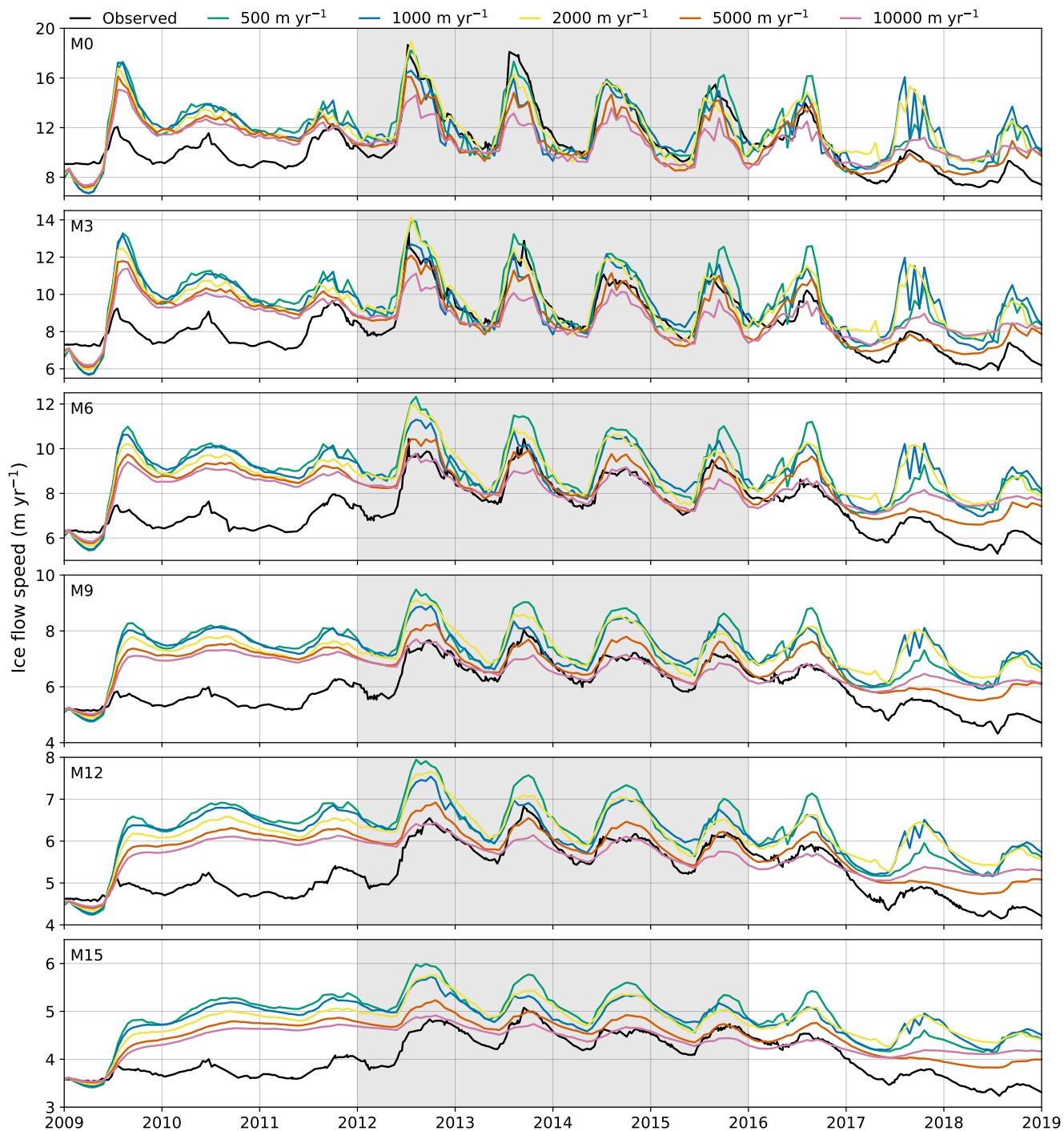
Figure S10. Time-series of observed (black line) and modelled (coloured lines) ice flow speeds at sites M0 to M15 for the regularised sliding law with a range of values of the fast-sliding speed u_0.
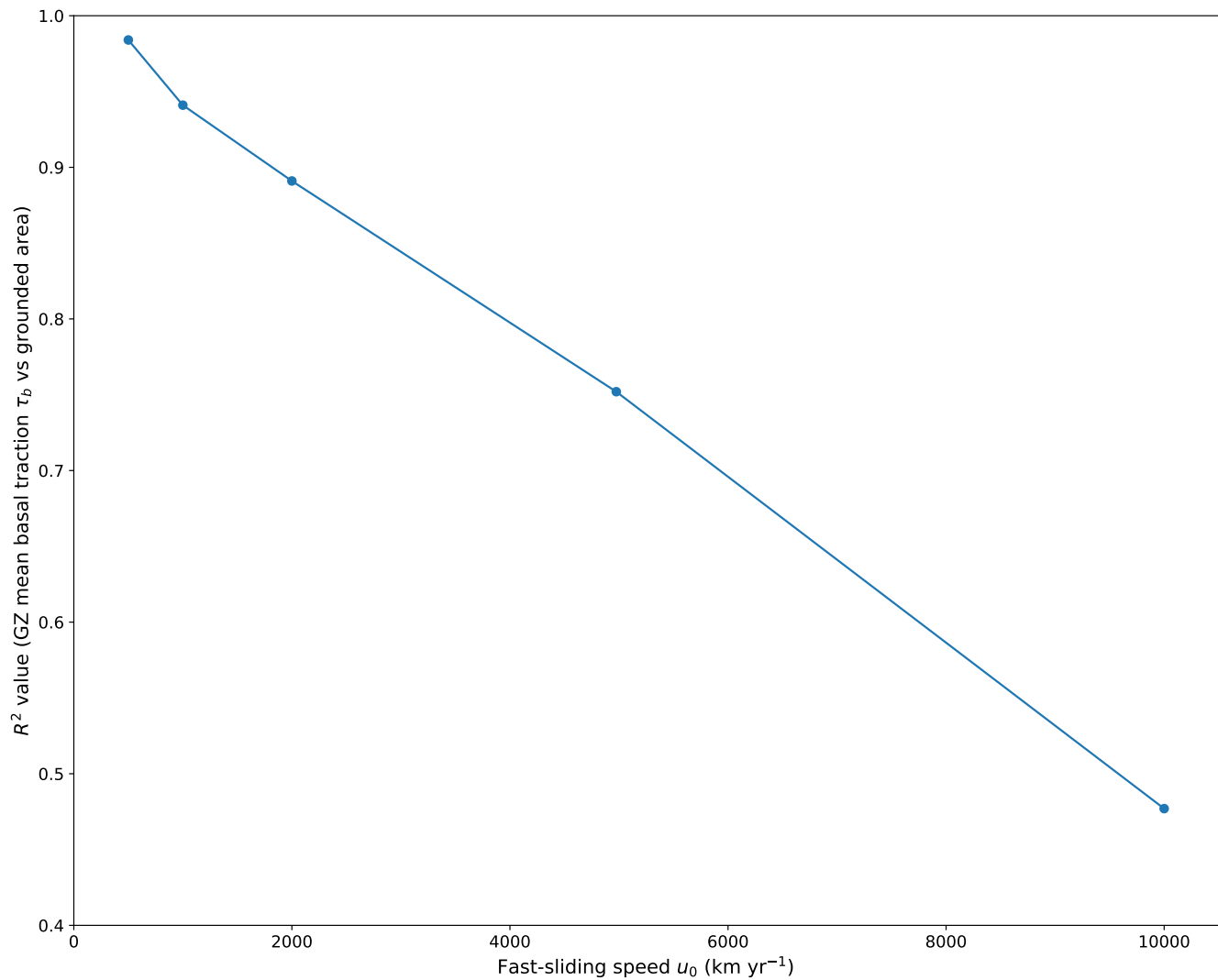
Figure S11. R-squared values for the linear relationship between mean basal traction and grounded area sampled within the GZ (e.g. Figure 7b and d) for a range of values of the fast-sliding speed u_0. R^2 was 0.21 for Weertman sliding law which effectively has $u_0 = \infty$.

References

Joughin, I.: MEaSUREs Greenland Monthly Ice Sheet Velocity Mosaics from SAR and Landsat, Version 1, https://doi.org/https://doi.org/10.5067/OPFQ9QDEUFFY, 2019.

Joughin, I., Smith, B. E., Howat, I. M., and Scambos, T. A.: MEaSUREs Greenland Ice Sheet Velocity Map from InSAR Data, Version 2, https://doi.org/https://doi.org/10.5067/OC7B04ZM9G6Q, 2018.

5   Joughin, I., Shean, D. E., Smith, B. E., and Floricioiu, D.: A Decade of Variability on Jakobshavn Isbrae: Ocean Temperatures Pace Speed Through Influence on Mélange Rigidity, The Cryosphere Discussions, pp. 1–27, https://doi.org/10.5194/tc-2019-197, 2019.

Joughin, I., Howat, I. M., Smith, B. E., and Scambos, T. A.: MEaSUREs Greenland Ice Velocity: Selected Glacier Site Velocity Maps from InSAR, Version 2, https://doi.org/https://doi.org/10.5067/JQHJUOYCF2TE, 2020.

10   Rignot, E. and Mouginot, J.: Ice flow in Greenland for the International Polar Year 2008-2009, Geophysical Research Letters, 39, 0–7, https://doi.org/10.1029/2012GL051634, 2012.